Springer

KSME

Journal of Mechanical Science and Technology 30 (5) (2016) 2019~2028
www.springerlink.com/content/1738-494x(Print)/1976-3824(Online)
DOI 10.1007/s12206-016-0408-y

Experimental study on variations in charpy impact energies of low carbon steel, depending on welding and specimen cutting method †

Zhaorui Yang, Hansaem Kang and Youngseog Lee*

Department of Mechanical Engineering, Chung-Ang University, Seoul 156-756, Korea

(Manuscript Received July 23, 2015; Revised October 31, 2015; Accepted December 29, 2015)

Abstract

This paper presents an experimental study that examines variations of Charpy impact energy of a welded steel plate, depending upon the welding method and the method for obtaining the Charpy specimens. Flux cored arc welding (FCAW) and Gas tungsten arc welding (GTAW) were employed to weld an SA516 Gr. 70 steel plate. The methods of wire cutting and water-jet cutting were adopted to take samples from the welded plate. The samples were machined according to the recommendations of ASTM SEC. II SA370, in order to fit the specimen dimension that the Charpy impact test requires. An X-ray diffraction (XRD) method was used to measure the as-weld residual stress and its redistribution after the samples were cut. The Charpy impact energy of specimens was considerably dependent on the cutting methods and locations in the welded plate where the specimens were taken. The specimens that were cut by water jet followed by FCAW have the greatest resistance-to-fracture (Charpy impact energy). Regardless of which welding method was used, redistributed transverse residual stress becomes compressive when the specimens are prepared using water-jet cutting. Meanwhile, redistributed transverse residual stress becomes tensile when the specimens are prepared using wire cutting.

Keywords: As-weld residual stress; Charpy impact energy; Residual stress redistribution; Water-jet cutting; Wire cutting

1. Introduction

Welding inevitably produces incompatible strains in the weldment, the Heat-affected zone (HAZ), and the base metal. Subsequently, as-weld residual stresses are generated. In this study, the area comprising the weldment, the HAZ, and the base metal near the HAZ is called the "weld zone" for convenience. Welding methods have been cause for concern among designers of large welded structures, since its fatigue behavior in service is influenced greatly by stress states at the weld zone. For example, as-weld tensile residual stresses in the weld zone directly reduce the resistance-to-failure of the large welded structure.

We should take the samples from the large welded structure to evaluate the effect of the as-weld residual stress on the resistance to failure of the weld zone. However, the samples cannot be cut out of the large welded structure, because the large welded structure is not made for testing purposes. As an alternative, small-sized steel plates (for example, 200 × 200 mm), are welded, and samples are cut from the welded steel plate. In this case, the as-weld residual stresses existing in the weld zone are redistributed in the course of cutting. The samples are then machined and reduced in size to the specimen dimension that the instrument (or experimental set-up) requires. As a result, the as-weld residual stresses, which are redistributed during cutting, are redistributed again in the course of machining. The terms "as-weld residual stress" and "residual stress" are used together throughout this paper for convenience.

Many experimental works and numerical studies have estimated the weld residual stress that is redistributed in the course of cutting and machining. Sridhar et al. [1] examined the residual stress deviation in titanium alloy IMI-834 as a function of depth, following milling at different feeds, speeds, and depths of cut. Ulutan et al. [2] proposed an analytical model for predicting the residual stresses in machining; the model was verified by comparing the predictions with the measurements on bearing steel 100Cr6 (JIS SUJ2). Navas et al. [3] measured residual distributions that were generated in quenched and tempered AISI O1 (F-522) tool steel by different machining processes: Electro-discharge machining (EDM), hard turning and grinding. They reported that EDM was the most harmful to the surface integrity. Arola and Ramulu [4] studied the effect of cutting parameters and material properties on the residual stress fields resulting from Abrasive water jet (AWJ) machining of materials (AISI 4340, AISI 304, A17075-T6, molybdenum). They found that the magnitude of

*Corresponding author. Tel.: +82 2 820 5256
E-mail address: ysl@cau.ac.kr
† Recommended by Associate Editor Choon Yeol Lee

Table 1. Chemical composition and mechanical properties of the base material and weld material.

	Materials	Typical chemical compositions			UTS	Yield strength	Elongation
		C	Si	Mn	N/mm²	N/mm²	%
Base material	SA516Gr.70	~0.28	0.15~0.4	0.85~1.2	485~620	260~	17~
Weld material	E91T1-B3 (FCAW)	~0.08	~0.62	~0.54	~726	604	19
	ER70S-2 (GTAW)	~0.07	0.4~0.7	0.9~1.4	540	410	25

residual stresses in the plane of the surface increased noticeably as the melting temperature of the weld material increased. Dattoma et al. [5] examined the evolution of residual stress fields that suffered due to chip-forming machining (such as milling and cutting) by comparing the measurements with finite element analysis results.

Altenkirch et al. [6] tried to establish guidelines for estimating the stress relaxation caused by sectioning welded plates in the longitudinal and transverse directions, respectively. Recently, Jiang et al. [7] investigated the characteristic distance, defined as the maximum length at which the as-weld stress is largely unchanged by a cutting length. They reported that the minimum cutting length to avoid the stress relaxation by cutting was approximately 6 times the characteristic length (66 mm) and about 12 times the plate thickness (25 mm). Liu et al. [8] performed a numerical and experimental study of welding residual stress redistribution of TA15 titanium plates joined by EWB. They reported that the transverse stress on the newly-formed surface decreased significantly, as compared to the as-welded stresses measured at the same locations when material on the top and bottom was removed.

These studies [1-8] did not draw a connection between the residual stress redistribution induced by cutting and machining and variations in the resistance-to-fracture of the weld zone. If the residual stresses redistributed in the preparation of the specimens are not understood, their effect on the resistance-to-fracture of the weld zone cannot be investigated thoroughly. In such a case, it is difficult to apply the test results (or computational results) to designs of large welded structures.

This paper examines the correlation between the residual stress redistribution induced by cutting and the resistance-to-fracture of the weld zone, by conducting a welding test and a Charpy impact test. Flux cored arc welding (FCAW) and Gas tungsten arc welding (GTAW) were employed to weld SA516 Gr.70 plates. Wire cutting (WC) and Water-jet cutting (WJC) were used to take the samples from the welded plate. After a set of samples were taken, the specimens were machined according to the recommendations of ASTM SEC. II SA370 (2010), fitting the specimen dimensions that the Charpy impact test requires. As-weld residual stress and stresses redistributed at each sample and specimen preparation stages were measured using the X-ray diffraction (XRD) method. The absorbed energy of the weld zone was measured by performing the Charpy impact test. Finally, the effect of residual stresses redistributed by cutting on the resistance-to-fracture of the weld zone was examined.

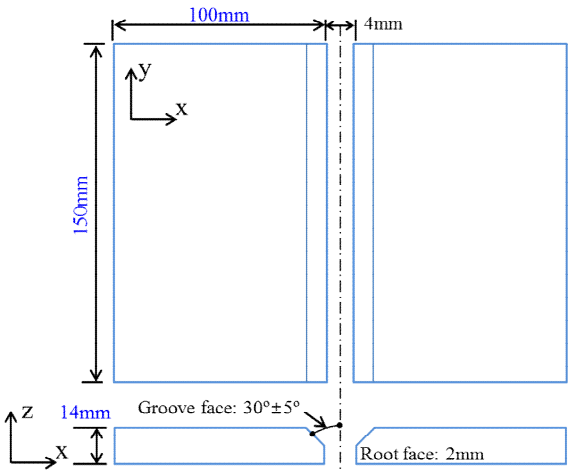

Fig. 1. Configuration of weld joint and dimensions of plates for welding.

2. Experimental

2.1 Materials

Plates of SA516Gr.70, usually used in the primary piping systems of nuclear power plants, are used as the parent (base) material. The thickness of the base material (the plate) is 14 mm, its width is 100 mm, and its length is 150 mm. The chemical composition and mechanical properties of the base material and weld material (filler material) are summarized in Table 1.

2.2 Welding process

The plates were joined by means of the GTAW and FCAW. The configuration of plates and dimensional details of the single-Y groove are shown in Fig. 1. For GTAW, a gas metal arc welding torch was followed by a wire feedstock. The welding had 7 passes and the temperature at each interval was kept at 165-170°C. Arc current was set at 200 A, and arc voltage was set at 17 V. A shielding gas, consisting of a mixture of 80% volume argon (Ar) and 20% volume carbon dioxide (CO_2), was used. ER70s-2 was used as a filler material for

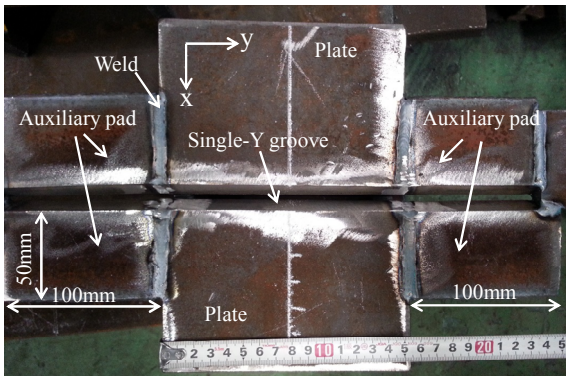

Fig. 2. Two plates are constrained by appropriate clampers at the transverse sides during the welding.

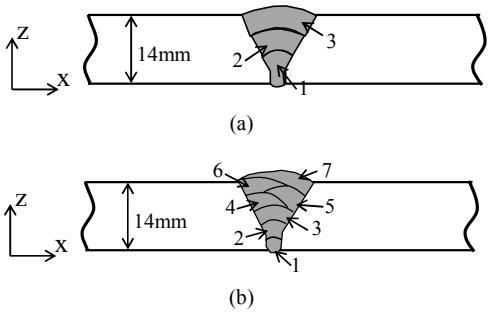

Fig. 3. Locations of the weld pass generated from: (a) Flux cored arc welding (FCAW); (b) Gas tungsten arc welding (GTAW).

GTAW. The supply rate that protects the weld pool was 20 L/min. The welding speed was kept constant at 1.4-1.6 mm/s.

FCAW had three passes, and temperature at each interval was kept 200-250°C. Arc current was set at 220 A, and arc voltage was set at 24 V. A shielding gas, carbon dioxide (CO_2), the filler material E91T1-B3 was supplied through the FCAW torch and used to protect the weld pool. The wire feed rate was kept constant at 33 mm/s and welding speed kept at 6 mm/s.

The two plates were restrained in the following manner. The plates were mounted on weld platforms and their bottom surfaces were tack-welded at four points. Fig. 2 shows a life-sized photograph of the two plates, together with four auxiliary steel pads, mounted on a weld platform before welding. In the pre-welding process, four auxiliary pads with 100 mm length were joined to the both ends of the plates to avoid sudden heat input at the both ends of the plates when the two plates were welded. The properties of the pad were the same as those of the plate. Preheating was applied along the single Y-groove region to eliminate the residual stress produced during the pre-welding process. The auxiliary pads were cut by a wheel saw after the welded plate (including the four auxiliary pads) was cooled to room temperature.

Fig. 3 shows the sequence of welding pass and the dimensional details of weld beads. Weld beads were laid parallel to the weld center line using the stringer bead technique [9].

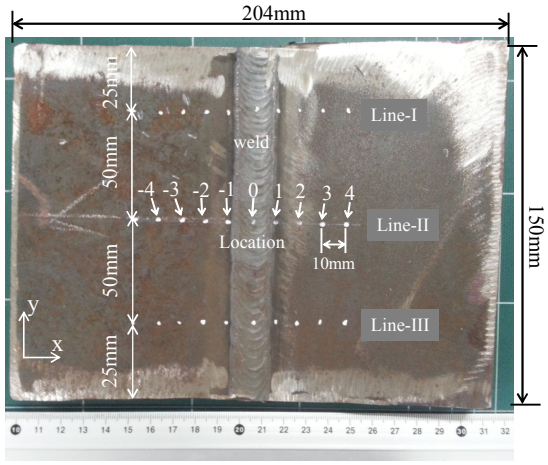

Fig. 4. A life-sized photograph of the welded plate, viewed from the top: (a) Plates are joined by GTAW; (b) plates are joined by FCAW. As-weld residual stresses are measured along Lines-I, II and III. The measurement points are marked with a set of white dots.

2.3 Residual stress measurement

X-ray diffraction (XRD), known as the "$\sin^2\psi$ - method [10]" was used to measure the residual stress. XSTRESS-3000, manufactured by the Stress Tech group [11], was used. The voltage and current applied were 20 KV and 2 mA, respectively. The beam was 2.54 mm in diameter and counting times of 40 seconds were used for peak [12].

Fig. 4 shows a life-sized photograph of a welded plate, viewed from the top. The locations that residual stresses were measured are indicated by a set of white dots. Each line has nine measurement points across the weld (weldment). Line-I and III, located near the end of the welded plate, were selected to examine the effect of location from which the specimens are taken in the welded plate on the redistribution of residual stresses. The numbers (-4, -3, -2, -1, 0, 1, 2, 3, 4) indicate the points that the residual stresses are measured along each lines. The distance between the points is 10 mm. A point "0"

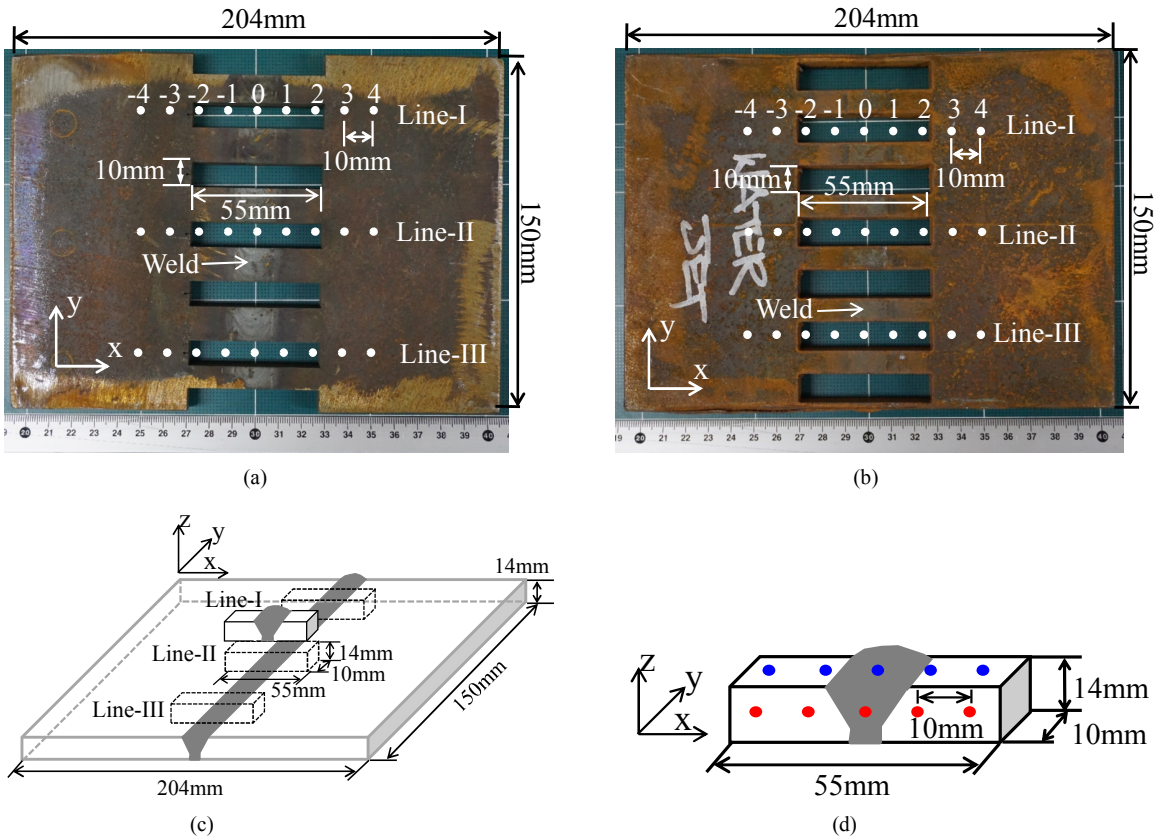

Fig. 5. A life-sized photograph of the welded plate from which the samples are taken by: (a) Wire cutting; (b) water-jet cutting; (c) 3D configurations of the samples taken by Wire cutting (WC) and Water-jet cutting (WJC); (d) the residual stress redistribution induced by cutting was measured at the five points on the cutting surface (marked with red dots) and the welding plane (marked with blue dots) of the sample.

marked with a white dot lies at the center of the weldment. Two points, "-1" and "1" are positioned around the Heat affected zone (HAZ). Four points, "-4", "-3", "3" and "4" are positioned on the base material. Two points, "-2" and "2" lie approximately between the HAZ and the base material.

2.4 Preparation of samples and specimens

A set of samples was taken from the welded plate after the as-weld residual stress was measured. An abrasive water-jet machine (BC-1212, Korea) and a wire cutting machine (EDM AP200L, Japan) were used to obtain the samples. Figs. 5(a) and (b) show a life-sized photograph of a welded plate from which samples were taken by Wire cutting (WC) (Fig. 5(a)) and Water-jet cutting (WJC) (Fig. 5(b)). The seven samples were cut out perpendicularly to the welding direction (y-axis). 3D configurations of the WC and WJC process are illustrated in Fig. 5(c). 3D configuration of a sample cut out of the welded plate is shown in Fig. 5(d). The residual stress redistributed by the WC and WJC was measured at five points (marked with red and blue spots) on the y-plane and the z-plane, respectively.

Figs. 6(a) and (b) show a life-sized photograph of the two cutting processes. Fig. 6(a) shows samples being taken by WC from a welded plate. A sample was already cut and fallen down. Fig. 6(b) shows that a number of samples were already cut by WJC.

In the wire-cutting process, the wire's diameter was 0.2 mm, and the gap between the wire surface and the cut-out material was set to 0.4 mm. The voltage and current applied were 100 V and 30 A, respectively. Wire tension was set to 20 N, and cutting speed was 0.03 mm/s. Meanwhile, cutting width of the water jet was 0.5 mm and nozzle water pressure was 38 MPa, respectively. Flow rate of abrasive water was 680 g/min, and cutting speed was 100 mm/min.

After the redistributed residual stresses in the samples were measured, the samples were machined into the specimen dimension that the Charpy impact test requires. Note that the samples prepared by WJC and WC have dimensions 14 × 10 × 55 mm since the thickness of the plate (SA516 Gr. 70) is 14 mm. Hence, a thickness of 14 mm was reduced to 10 mm, as the latter is the dimension that the Charpy test requires (a rectangular specimen: 10 × 10 × 55 mm). Along the z-axis, a horizontal milling machine cuts 2 mm below the upper surface level and 2 mm above the lower surface level of the samples.

Residual stresses in the specimen are redistributed again by milling process. But the secondary residual stress redistributions in the specimens were not measured before the Charpy

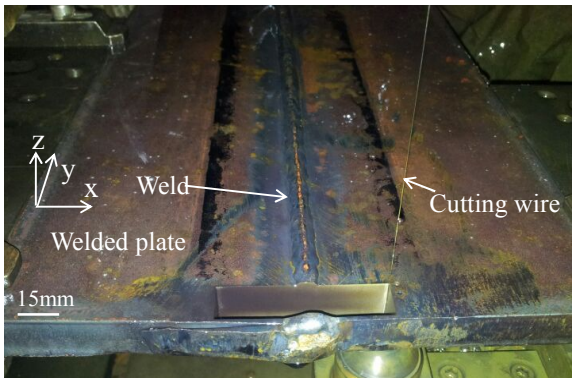

(a)

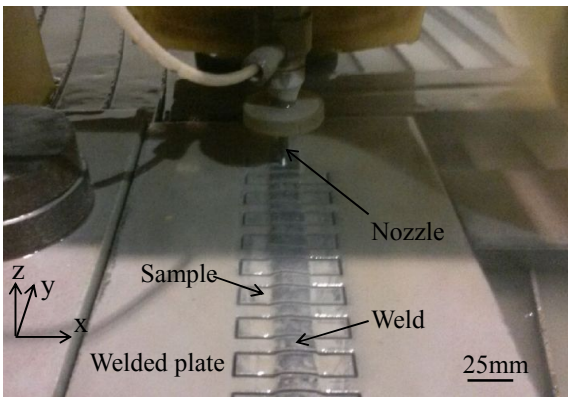

(b)

Fig. 6. A life-sized photograph of a cutting process: (a) A sample is taken by WC. A sample was already cut and fallen down; (b) several samples were taken by WJC.

impact test began. It is because Liu et al. [8] reported the variation pattern of the through thickness redistributed transverse residual stresses is similar to that of the as-weld residual stress with material removed from the thickness, and the magnitude of residual stresses is decreased slightly. In this light, we assumed that the variation pattern of redistributed transverse residual stresses in the samples (obtained by cutting after welding) is similar to that in the specimens (obtained by cutting and milling after welding), and a change in the redistributed residual stresses is insignificant if a small part of the sample thickness is removed by milling.

2.5 The Charpy test

The Charpy V-notch (CVN) impact test is one of standardized test methods that quickly evaluate a material's resistance-to-fracture. In this study, the Charpy test was performed according to standard test methods (ASTM SEC. II SA370: 2010). The total length of the specimen is 55 mm, and the rectangular cross-section area is 10 × 10 mm. The specimen has a V-shaped notch with a flank angle of 45° and depth of 2 mm. The tip radius of the notch is 0.25 mm, and the radius of the striking edge is 8 mm.

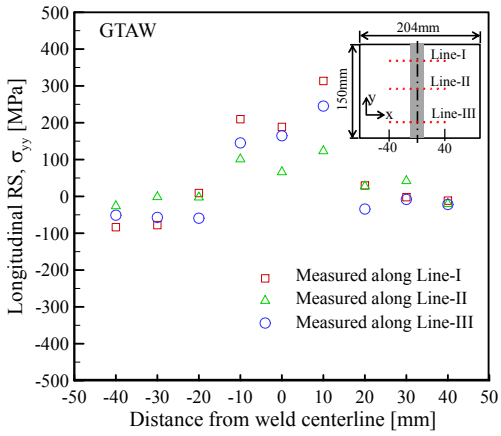

(a)

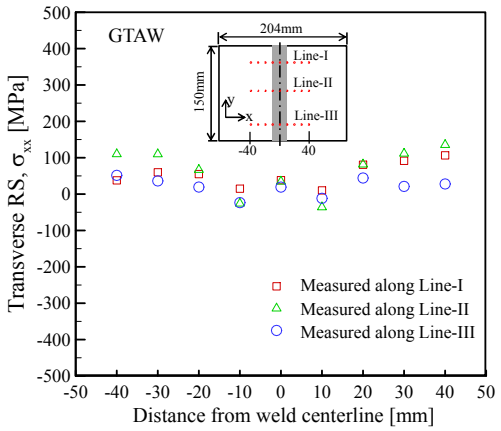

(b)

Fig. 7. Variations in as-weld RS along each line after the plates were joined by GTAW: (a) As-weld RS toward the direction of welding; (b) as-weld RS perpendicular to the welding direction. The nine points marked with red dots correspond to the points marked with white dots explained in Fig. 4. The distance between the points is 10 mm.

3. Results and discussion

3.1 As-weld residual stress by GTAW

Fig. 7 shows the measured as-weld residual stresses produced by GTAW. The area marked with grey (shown at the upper right of the Fig. 7) denotes the weld (weldment). Hereafter, the as-weld residual stress is called "RS" for convenience. RS were measured at nine points (marked with red dots) along three lines (Lines-I, II and III). The nine points correspond to the measurement locations explained in Fig. 4. Variations in RS along Line-II are different from those along Line-I and Line-III, since the Line-I and Line-III are close to the edge of the plate.

In Fig. 7(a), longitudinal RS (σ_{yy}) at the weld along Line-I and Line-III reaches approximately 200 MPa on average, but that at the weld along Line-II is about 100 MPa. The difference is attributable to the fact that the cooling rate at Line-I and Line-III is faster than that at Line-II after the welding process is completed. Meanwhile, maximum longitudinal

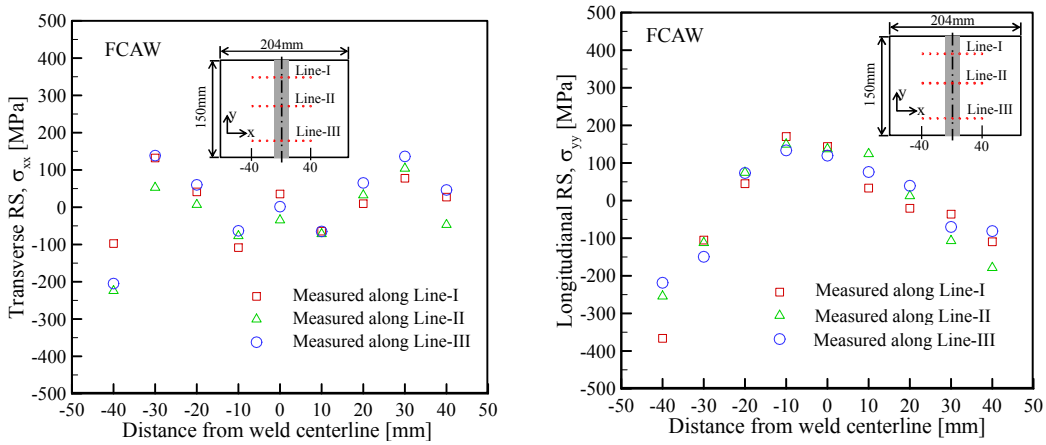

Fig. 8. Variations in as-weld RS along each line after the plates were joined by FCAW: (a) As-weld RS toward the direction of welding; (b) as-weld RS perpendicular to the welding direction. The nine points marked with red dots correspond to the points marked with white dots explained in Fig. 4. The distance between the points is 10 mm.

tensile RS occurs near the interface of the weld and the HAZ (at about ±10 mm from the weld centerline). Similar results were reported by Kim et al. [13]. They joined 9Cr-1 Mo steel plates using GTAW and measured RS with a neutron diffraction method. They also reported that the maximum longitudinal tensile RS occurred near the interface between the weld and the HAZ.

Fig. 7(b) shows transverse RS (σ_{xx}) along the three lines. In contrast to the longitudinal RS, the end effect on the transverse RS is strong at the base material rather than the weld. A maximum difference of the transverse RS at the weld is about 38 MPa. On the other hand, a maximum difference of the transverse RS at the base material increases to 135 MPa. This finding might be attributable to the fact that the constraint condition (clamping condition on the weld platform) along the *x*-axis is much stronger than that along the *y*-axis. Leggatt's work also reported this type of as-weld RS profile due to the constraint condition [14]. When the transverse RS are measured crossing the middle of the welded plate (along Line-II), the transverse RS on the left-hand side and that on the right-hand side are somewhat balanced. However, the transverse RS along Line-I and Line-III are slightly out of balance, indicating that the plates were not perfectly clamped in balance towards the transverse direction in the pre-welding process.

3.2 As-weld residual stress by FCAW

Fig. 8(a) shows longitudinal RS when the plates are joined by FCAW. The area marked with grey denotes the weld. In a similar manner as discussed in Sec. 3.1, RS were measured at nine points along three lines (Lines-I, II and III). The nine points marked with red dots correspond to the locations explained in Fig. 4. Variations of longitudinal RS across the weld have a similar pattern of longitudinal RS generated by GTAW (see Fig. 7(a)). However, magnitude of RS (both tensile and compressive) produced by FCAW is about 14% greater than that generated by GTAW because the heat input (1200 J/mm) of FCAW is much greater than that (840 J/mm) of GTAW.

Fig. 8(b) shows the transverse RS across the weld produced by FCAW. Its variation pattern is M-shaped. Paradowska et al. [15] reported this kind of profile when low-carbon steel plates were joined using FCAW. Variation pattern in the transverse RS shown in Fig. 8(b) is greater than those in Fig. 7(b). This is because the transverse RS is affected by a wide range of factors, including the geometry of the joined part and the pass sequence for multi-pass welds [14].

3.3 Redistribution of as-weld Residual stress (RS)

After the welded plate was cooled completely to room temperature, a set of samples was taken from the welded plate using WJC and WC. As-weld residual stress in the samples is redistributed by the process of WJC and WC. The locations from which the samples are taken, and their dimensions, were explained in Fig. 5(c). Explanations of the measurement points (five points marked with blue and red dots) are given in Fig. 5(d).

Fig. 9(a) shows the redistributed transverse RS on the welding surface (*z*-plane) after the samples were taken out of the plate that was welded by GTAW. Note that the redistributed longitudinal RS was not measured in this study since its direction was parallel to the impact line in the Charpy specimen. If the direction of redistributed longitudinal RS and the impact line are positioned in a parallel direction, the redistributed longitudinal RS has little effect on the resistance-to-fracture of the Charpy specimen. A comparison of Fig. 7(b) (as-weld transverse RS) and Fig. 9(a) (redistributed transverse RS) reveals that the as-weld transverse RS decreases by merely 3.05% on average after it is redistributed. This is because the

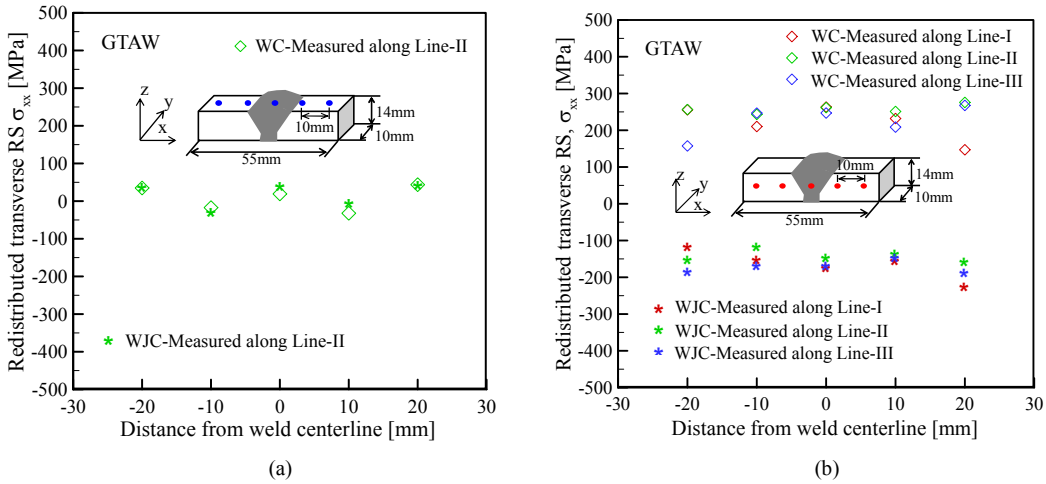

Fig. 9. Redistributed transverse RS after the plates were joined by GTAW and after specimens were taken from the welded plate by WC and WJC. The five points marked with blue and red dots correspond to the points marked with blue and red dots explained in Fig. 5(d): (a) Redistributed transverse RS was measured on the welding plane (*z*-plane); (b) redistributed transverse RS was measured on the cutting surface (*y*-plane).

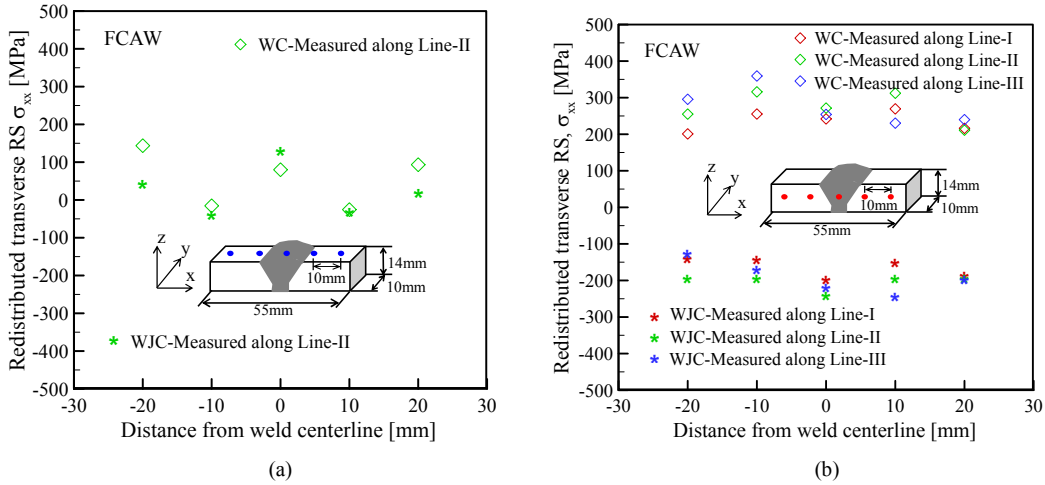

Fig. 10. Redistributed transverse RS after the plates were joined by FCAW and after specimens were taken from the welded plate by WC and WJC. The five points marked with blue and red dots correspond to the points marked with blue and red dots explained in Fig. 5(d): (a) Redistributed transverse RS was measured on the welding plane (*z*-plane); (b) redistributed transverse RS was measured on the cutting surface (*y*-plane).

characteristic distance (a length along transverse direction of the welded plate) is over three times longer than the length of the sample taken out of the welded plate. This fact was confirmed by Prime et al's work [16]. They reported that residual stress is reduced by only 2% if the characteristic distance is twice or three times longer than the dimension, i.e., the length of the sample.

Fig. 9(b) shows that redistributed transverse RS on the cutting surface (*y*-plane) is influenced significantly by a cutting method. The redistributed transverse RS induced by WC becomes tensile, but the redistributed transverse RS induced by WJC becomes compressive. The following studies confirm these trends. Navas et al. [3] reported that Wire electro-discharge machining (WEDM) generated tensile stresses at the cutting surface. Arola et al. [4] also observed that the wire-jet cutting resulted in compressive residual stress at the cutting surface. It is difficult to distinguish between the weld region and the base region from the measurement data of redistributed transverse RS. The differences grow smaller among redistributed transverse RS along Lines-I, II and III, respectively.

Fig. 10(a) shows the redistributed transverse RS on the welding surface (*z*-plane) after the samples were taken out of the plate welded by FCAW. A comparison of Fig. 8(b) (as-weld transverse RS) and Fig. 10(a) (redistributed transverse RS) demonstrates that as-weld transverse RS is decreased by only 2.6% on average after it is redistributed. The reason for such a small decrease has been explained above.

Fig. 10(b) shows the redistributed transverse RS on the cutting surface (*y*-plane). As in Fig. 9(b), the cutting process (WJC and WC) influences considerably the redistributed transverse RS. However, in the sample taken out of the plate welded by FCAW, the magnitude of the redistributed trans-

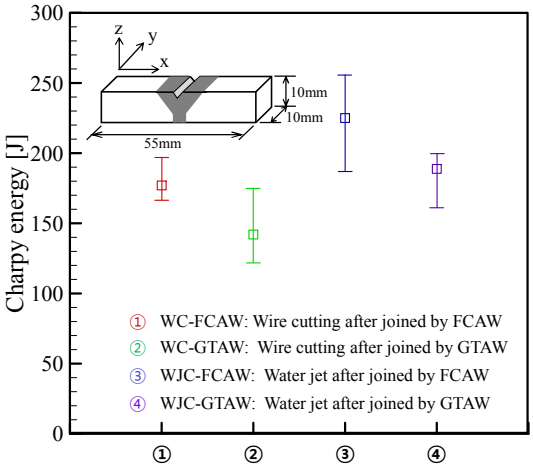

Fig. 11. Variations in the Charpy energy, dependent upon the welding method and cutting method. The numbers inside the circle in the *x*-axis denote the cutting method and welding method.

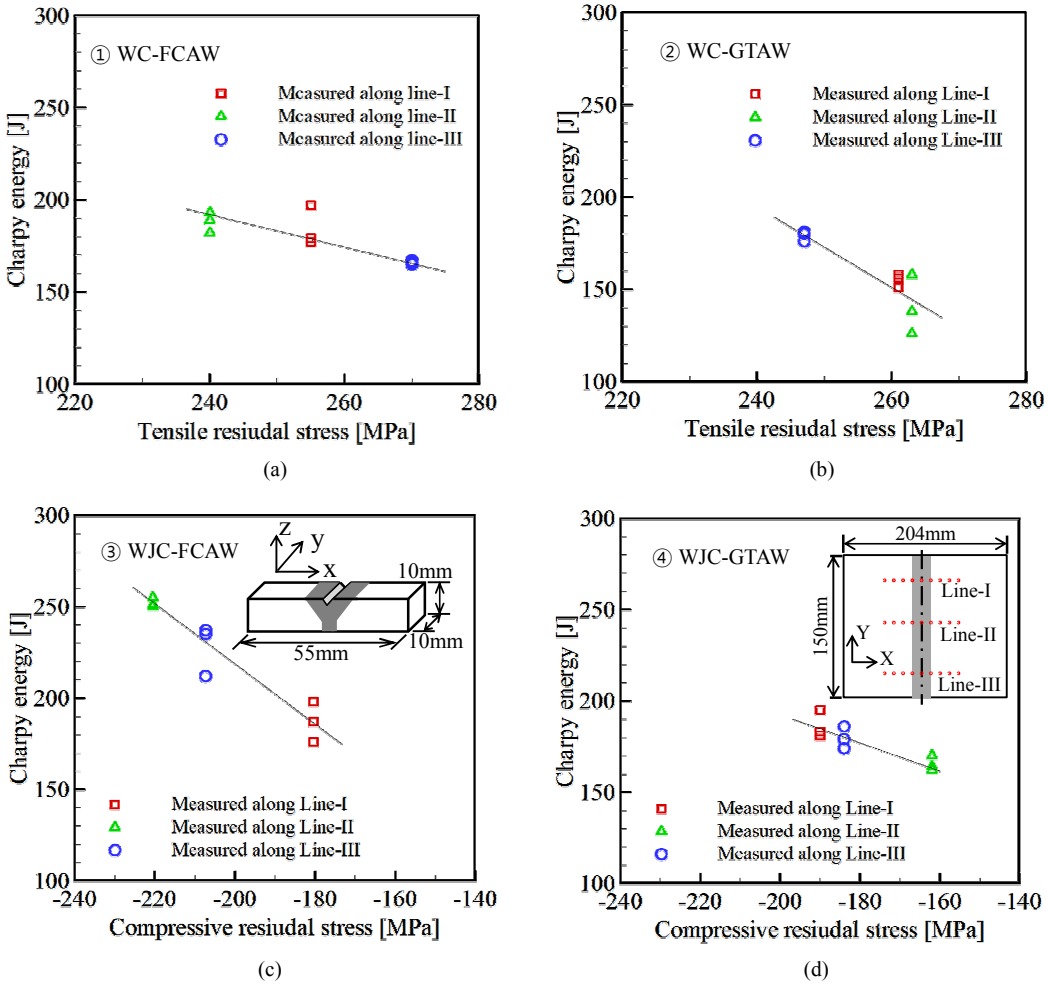

Fig. 12. The relationship between the Charpy energy and the magnitude of the redistributed RS dependent on the locations (Lines-I, II and III) from which the specimens are taken in the welded plate. The numbers inside the circle in the *x*-axis denote the cutting method and welding method.

verse RS is slightly larger than that from the plate welded by GTAW. This finding is because the weld plate was joined by FCAW, which uses strong weld material (yield stress 604 MPa, UTS 726 MPa).

3.4 The Charpy energy

The effect of residual stress redistribution caused by WC and WJC on the resistance-to-fracture, which is usually expressed as the energy that the specimen absorbs during test, was examined. Hereafter, the energy that the specimen absorbs during the test is called "Charpy energy" for convenience.

Fig. 11 shows variations in the Charpy energy depending on the welding process (GTAW and FCAW) and on the cutting process (WC and WJC). The number inside the circle in the *x*-axis denotes the cutting process and the welding process. For example, "①" denotes a case where the plates are joined by FCAW and then the specimens are taken from the welded plate by WC. Nine specimens are used for each case.

The effect of a cutting process on the Charpy energy is observed by comparing "①" with "③", and by comparing "②" with "④". Water-jet cutting leads to greater Charpy energy than WC, regardless of the type of welding process. This is because compressive stresses remain in the specimen obtained by water jet, but tensile stresses remain in the specimen obtained by wire cut.

In a similar manner, the effect of a welding process on the Charpy energy is examined by comparing "①" with "②", and by comparing "③" with "④". The difference is attributable to the fact that the stronger weld material (yield stress 604 MPa, UTS 726 MPa) was used for FCAW. Therefore, the Charpy energy is greatest for case "③". It denotes that these cases (in which the specimens were made by water jet and the plates were joined by FCAW) have the greatest resistance-to-fracture.

Fig. 12 shows the relationship between the Charpy energy and the magnitude of redistributed RS dependent on the locations (Lines-I, II and III) from which the specimens are taken from the welded plate. The circled numbers in Figs. 12(a)-(d) denote different welding and cutting combinations, as explained above. In all cases, the Charpy energy is markedly dependent on the locations from which the specimens are taken from the welded plate. The Charpy energies in Figs. 12(a) and (b) are less than those in Figs. 12(c) and (d), since tensile RS remains in the specimens following welding (GTAW and FCAW) and cutting (WC and WJC). Fig. 12(c) shows that the Charpy energy is greatest when the specimen was taken on line-II. This is because redistributed compressive RS was induced on the cutting surface of the specimens by WJC, and the weld plate was joined by FCAW, which uses strong weld material. Meanwhile, the Charpy energy in Fig. 12(d) was low, although redistributed compressive RS remained in the specimen, because the strength of the weld material used in GTAW is low compared with that in FCAW. In summary, when the specimens were cut by WC, the difference ranged from -7.7% to 20.4%. On the other hand, the difference is in the range of -14.8% to 6.6% when the specimens were cut by WJC.

4. Concluding remarks

By means of welding tests and the Charpy impact tests, this study examined a correlation between the residual stress redistribution induced by cutting and the resistance-to-fracture of the weld zone. Flux cored arc welding (FCAW) and Gas tungsten arc welding (GTAW) were employed to weld SA516 Gr. 70 plates. Wire cutting (WC) and Water-jet cutting (WJC) were adopted to take the specimen from the welded plate. The absorbed energy of the weld zone was measured by performing the Charpy impact test. The effect of residual stresses redistribution by cutting on the resistance-to-fracture was investigated. The conclusions are as follows:

(1) Redistributed transverse residual stress becomes compressive when the specimens are taken out of the plate welded by WJC. Meanwhile, redistributed transverse residual stress becomes tensile when the specimens are taken out of the plate welded by wire jet.

(2) When the plates are welded by FCAW, the Charpy energy of the specimen prepared by WJC is 25.2% larger than that by WC. Meanwhile, the Charpy energy of the specimen made by WJC is 30.3% larger than that by WC when the plates are welded by GTAW. Higher Charpy energy of the specimen prepared by FCAW might be attributable the weld material (E91T1-B3) which has higher UTS and yield strength than the weld material (ER70S-2).

(3) The Charpy energy of the specimens is significantly dependent on the locations (Lines-I, II and III) of the welded plate where the specimens are taken. Hence, the specimens taken from the welded plate should not be in the narrow region when we prepare the specimen for the weld test.

(4) The Charpy energy has the greatest value, on average, when the specimens are taken by water jet after the plates are welded by FACW.

Acknowledgement

This research was supported by Basic Science Research Program through the National Research Foundation of Korea (NRF) funded by the Ministry of Education (2012R1A1A2006433).

Reference

[1] B. R. Sridhar, G. Devanda and K. Ramachandra, Effect of machining parameters and heat treatment on the residual stress distribution in titanium alloy IMI-834, *J. Mater. Proc. Tech*., 139 (2003) 628-634.

[2] D. Ulutan, E. B. Alaca and I. J. Lazoglu, Analytical modelling of residual stresses in machining, *J. Mater Proc. Tech*., 183 (2007) 77-87.

[3] V. G. Navas, I. Ferreres, J. A. Maranon, C. G. Rosales and J. G. Sevillano, Electro-discharge machining (EDM) versus hard turning and grinding-Comparison of residual stresses and surface integrity generated in AISI O1 tool steel, *J. Mater. Proc. Tech*., 195 (2008) 186-194.

[4] D. Arola and M. Ramulu, Material removal in abrasive water jet machining of metals A residual stress analysis, *Wear*, 211 (1997) 302-310.
[5] V. Dattoma, M. D. Giorgi and R. Nobile, On the evolution of welding residual stress after milling and cutting machining, *Comp. Struct*., 84 (2006) 1965-1976.
[6] J. Altenkirch, A. Steuwer, M. J. Peel and P. J. Withers, The extent of relaxation of weld residual stresses on cutting out cross-weld test-pieces, *JCPDS-International center for diffraction data* (2009) 593-607.
[7] W. Jiang, W. Woo, G. B. An and J. U. Park, Neutron diffraction and finite element modeling to study the weld residual stress relaxation induced by cutting, *Mater. Design*, 51 (2013) 415-420.
[8] C. Liu, J. Zhang, B. Wua and S. Gong, Numerical investigation on the variation of welding stresses after material removal from a thick titanium alloy plate joined by electron beam welding, *Mater. Design*, 34 (2012) 609-617.
[9] T. Kannan and N. Murugan, Effect of flux cored arc welding process parameters on duplex stainless steel clad quality, *J. Mater. Proc. Tech*., 176 (1) (2006) 230-239.
[10] V. I. Monin, R. T. Lopes, S. N. Turibus, J. C. Payao Filho and J. T. D. Assis, X-Ray diffraction technique applied to study of residual stresses after welding of duplex stainless steel plates, *Mater. Res*., 17 (2014) 64-69.
[11] Stress tech Oy FINLAND, *www. Stresstechgroup.com*.
[12] C. N. Ismail and B. C Jerome, *Residual stress-measurement by diffraction and interpretation*, Springer Science+Business Media, LLC (1987).
[13] S. H. Kim, J. B. Kim and W. J. Lee, Numerical prediction and neutron diffraction measurement of the residual stresses for a modified 9Cr-1Mo steel weld, *J. Mater. Proc. Tech*., 209 (8) (2009) 3905-3913.
[14] R. H. Leggatt, Residual stresses in welded structures, *Int. J. Pressure Vessels Piping*, 85 (3) (2008) 144-151.
[15] A. Paradowska, J. W. H. Price, R. Ibrahim and T. Finlayson, A neutron diffraction study of residual stress due to welding, *J. Mater. Proc. Tech*., 164 (2005) 1099-1105.
[16] M. B. Prime, T. G. Herold, J. A. Baumann, R. J. Lederich, D. M. Bowden and R. J. Sebring, Residual stress measurements in a thick, dissimilar aluminum alloy friction stir weld, *Acta. Mater*., 54 (15) (2006) 4013-4021.

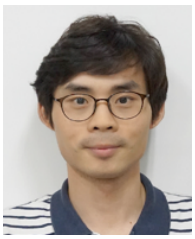

Zhaorui Yang received the B.S. in Mechanical Engineering from Kongju National University, Korea, in 2010. He then received the M.S. and Ph.D. degrees from Chung-Ang University, Seoul, Korea, in 2012 and 2016, respectively. His research interests include the finite element analysis and experiment of variations in the crack propagation direction and path in the welded joints of gas pipes. He is also interested in the warm shot peening process.

Youngseog Lee received the B.S. in Mechanical Engineering from Pusan National University, Korea, in 1989. He then received the M.S. and Ph.D. degrees from Case Western Reserve University, Cleveland, Ohio, USA, in 1992 and 1997, respectively. Until 2003, he worked as a researcher at POSCO Technical Research Laboratories, Pohang, Korea. He is currently a Professor in the Department of Mechanical Engineering, Chung-Ang University, Seoul, Korea. He is interested in numerical analysis of variations in the crack propagation direction and path of the welded joints of gas pipes.